

“A Research on Blade Pitch Control for Wind Mill”

Manoj Badgujar¹, Pankaj Patil², Gopal Patil³, Prof. B. M. Patil⁴

UG Scholar, Department of Electrical Engineering, SJRIT, Dondaicha, Maharashtra, India¹

Assistant Professor, Department of Electrical Engineering, SJRIT, Dondaicha, Maharashtra, India²

Abstract— The framework we considered is controlled to generate maximum vitality while limiting loads. The maximization of vitality was just carried out on a static basis and on ly drive train loads were considered as a constraint. In medium wind speeds, the generator and power converter control the twist turbine to capture maximum vitality from the wind. In the high wind speed area, the wind turbine is controlled to maintain the aerodynamic power created by the wind turbine. Two techniques to adjust the aerodynamic power were investigated: pitch control and generator load control, both of which are utilized to control the operation of the wind turbine. Our analysis and simulation demonstrates that the wind turbine can be operated at its ideal vitality capture while limiting the load on the twist turbine for an extensive variety of wind velocities. We survey the destinations and procedures utilized as a part of the control of horizontal axis twist turbines at the individual turbine level, where controls are applied to the turbine blade pitch and generator. The turbine framework is demonstrated as an adaptable structure operating within the sight of turbulent wind disturbances. Some review of the various stages of turbine operation and control strategies used to maximize vitality capture in beneath rated wind velocities is given, yet emphasis is on control to alleviate loads when the turbine is operating at maximum power. After checking on basic turbine control targets, we give a diagram of the regular basic linear control approaches and then portray more advanced control architectures and why they may give significant advantages.

Keywords— Foreground saliency, traffic sign, graph-based manifold ranking, a close-loop graph, foreground and background cues.

I. INTRODUCTION

The task of saliency disclosure for traffic sign is to perceive the most important and informative part of a scene. It has been applied to various vision issues including image segmentation, challenge acknowledgment, image weight, content based image retrieval [8], to name a couple. Saliency methods in general can be categorized as either base up or best down approaches. Base up methods are data-driven and pre-attentive, while best down strategies are task driven that entails managed learning with class labels. We take note of that saliency models have been created for eye fixation expectation and salient dissent acknowledgment. The past concentrates on perceiving two or three human fixation locations on natural images, which is important for understanding human attention. The latter is to accurately distinguish where the salient challenge should be, which is useful for many abnormal state vision tasks.

The main observation is that the distance between a pair of background areas is shorter than that of an area from the salient challenge and a locale from the background. The center point labeling task (either salient challenge or background) is formulated as a vitality minimization issue based on this criteria. We watch that background regularly demonstrates local or global appearance availability with each of four image boundaries and foreground presents appearance rationality and consistency. In this work, we abuse these cues to figure pixel saliency based on the ranking of superpixels. For each image, we build up a close-loop graph where each center point is a superpixel. We demonstrate saliency location as a manifold ranking issue and propose a two-stage contrive for graph labeling. Figure 1 demonstrates the main steps of the proposed algorithm. In the principal stage, we abuse the boundary earlier [13, 22] by

using the center points on each side of image as labeled background questions. From each labeled result, we figure the saliency of center points based on their relevances (i.e, ranking) to those inquiries as background labels. The four labeled maps are then integrated to generate a saliency map. In the second stage, we apply binary segmentation on the came about saliency map from the primary stage, and take the labeled foreground centers as salient inquiries. The saliency of each center is handled based on its relevance to foreground inquiries for the final map. To totally capture innate graph structure information and incorporate local gathering cues in graph labeling, we use manifold ranking systems to learn a ranking capacity, which is essential to learn an optimal affinity matrix [20]. Extraordinary in relation to [12], the proposed saliency acknowledgment algorithm with manifold ranking requires just seeds from one class, which are initialized with either the boundary priors or foreground cues. The boundary priors are proposed pushed on the present works of human fixations on images [31], which demonstrates that humans tend to gaze at the focal purpose of images. These priors have also been used as a part of image segmentation and related issues [13, 22, 34]. In contrast, the semi-coordinated method [12] requires both background and salient seeds, and generates a binary segmentation. Additionally, it is hard to choose the number and locations of salient seeds as they are generated by random walks, especially for the scenes with various salient articles. This is a known issue with graph labeling where the results are delicate to the picked seeds. In this work, all the background and foreground seeds can be easily generated via background priors and ranking background inquiries (or seeds). As our model incorporates local gathering cues extracted from the entire image, the proposed algorithm generates especially characterized boundaries of salient articles and reliably highlights the whole salient areas. Experimental results using large benchmark data sets demonstrate that the proposed algorithm performs adequately and favorably against the state-of-the-art saliency identification strategies.

II.LITERATURE SURVEY

In this paper, we concentrate on the base up salient question acknowledgment tasks. Salient dissent identification algorithms usually generate skipping boxes, binary foreground and background segmentation, or saliency maps which indicate the saliency probability of each pixel. Liu et al. [23] propose a binary saliency estimation demonstrate via training a conditional random field to join an arrangement of novel features. Wang et al. [32] analyze various cues in a united vitality minimization framework and use a graph-based saliency indicate [14] to perceive salient articles. In [24] Lu et al. develop a hierarchical graph demonstrate and utilize concavity setting to enlist weights between center points, from which the graph is bi-partitioned for salient question revelation. On the other hand, Achanta et al. [1] enroll the saliency probability of each pixel based on its shading contrast to the entire image. Cheng et al. [9] consider the global area contrast as for the entire image and spatial relationships across the locales to extract saliency map. In [11] Goferman et al. propose a setting aware saliency algorithm to recognize the image areas that speak to the scene based on four standards of human visual attention. The contrast of within and encompass circulation of features is handled based on the Kullback-Leibler disparity for salient question identification [21]. Xie et al. [35] propose a novel model for base up saliency inside the Bayesian framework by abusing low and mid level cues. Sun et al. [30] enhance the Xie's model by showing boundary and delicate segmentation. As of late, Perazzi et al. [27] demonstrate that the total contrast and saliency estimation can be formulated unifiedly using high-dimensional Gaussian channels. In this work, we generate a full-determination saliency map for each information image. Most above-said systems measure saliency by measuring local concentration encompass contrast and rarity of features over the entire image. In contrast, Gopalakrishnan et al. [12] formulate the dissent location issue as a binary segmentation or labeling task on a graph. The most salient seed and several background seeds are recognized by the behavior of random walks on a total graph and a k-regular graph. At that point, a semi-coordinated learning technique is used to incite the binary labels of the unlabelled centers. As of late a system that adventures background priors is proposed for saliency acknowledgment [34].

III. PROBLEM DEFINITIONS

The approaches for choosing low-level saliency can be based on biological models or absolutely computational ones. Some approaches consider saliency more than several scales while others operate on a solitary scale. In general, all strategies use a couple means of choosing local contrast of image areas with their surroundings using at least one of the features of shading, power, and orientation. Usually, separate feature maps are created for each of the features used and then joined [8, 11, 6, 4] to obtain the final saliency map. A whole survey of all saliency identification and segmentation research is past the degree of this paper, here we talk about those approaches in saliency acknowledgment and saliency-based segmentation that are most relevant to our work. Ma and Zhang [11] propose a local contrast-based strategy for generating saliency maps that operates at a solitary scale and is not based on any biological model. The commitment to this local contrast-based map is a resized and shading quantized CIELuv image, sub-separated into pixel squares. The saliency map is obtained from summing up yielding's of image pixels with their separate encompassing pixels in a small neighborhood. This framework extracts the concentrations and areas of attention. A cushy creating system then parts salient regions from the saliency map. Hu et al. [6] create saliency maps by thresholding the shading, drive, and orientation maps using histogram entropy thresholding analysis instead of a scale space approach. They then use a spatial compactness measure, figured as the area of the raised body encompassing the salient region, and saliency thickness, which is a segment of the magnitudes of saliency values in the saliency feature maps, to measure the individual saliency maps before consolidating them. Itti et al. [9] have developed a computational model of saliency-based spatial attention gotten from a biologically plausible architecture. They figure saliency maps for features of luminance, shading, and orientation at deferent scales that aggregate and consolidate information about each location in an image and sustain into a joined saliency map in a base up manner. The saliency maps conveyed by Itti's approach have been used by various researchers for applications like adapting images on small gadgets [3] and unsupervised question segmentation [5, 10]. Segmentation using Itti's saliency maps (a 480x320 pixel image generates a saliency map of size 30x20 pixels) or any other sub-sampled saliency map from a deferent strategy requires complex approaches. For instance, a Markov random field model is used to integrate the seed values from the saliency map along with low-level features of shading, surface, and edges to build up the salient dissent locale [5]. Ko and Nam [10], on the other hand, use a Support Vector Machine trained on the features of image segments to pick the salient locales of enthusiasm from the image, which are then packed to extract the salient articles. We demonstrate that using our saliency maps, salient dissent segmentation is conceivable without requiring such complex segmentation algorithms. As of late, Frintrop et al. [4] used integral images [14] in VOCUS (Visual Object Detection with a Computational Attention System) to accelerate computation of center encompass regard's for Finding salient areas using separate feature maps of shading, constrain, and orientation. Although they obtain better determination saliency maps as compared to Itti's procedure, they resize the feature saliency maps to a lower scale, along these lines losing determination. We use integral images in our approach anyway we resize the Filter at each scale instead of the image and henceforth maintain the same determination as the original i.

IV. PROPOSED SOLUTION

The AT89C51 is a low-power, high-performance CMOS 8-bit microcomputer with 4 bytes of Flash Programmable and Erasable Read Only Memory (PEROM). The device is manufactured using Atmel's high density non-volatile memory technology and is compatible with the industry standard MCS-51™ instruction set and pin out. The on-chip Flash allows the program memory to be reprogrammed in-system or by a conventional non-volatile memory programmer. By combining a versatile 8-bit CPU with Flash on a monolithic chip, the Atmel AT89C51 is a powerful microcomputer, which provides a highly flexible and cost effective solution to many embedded control applications.

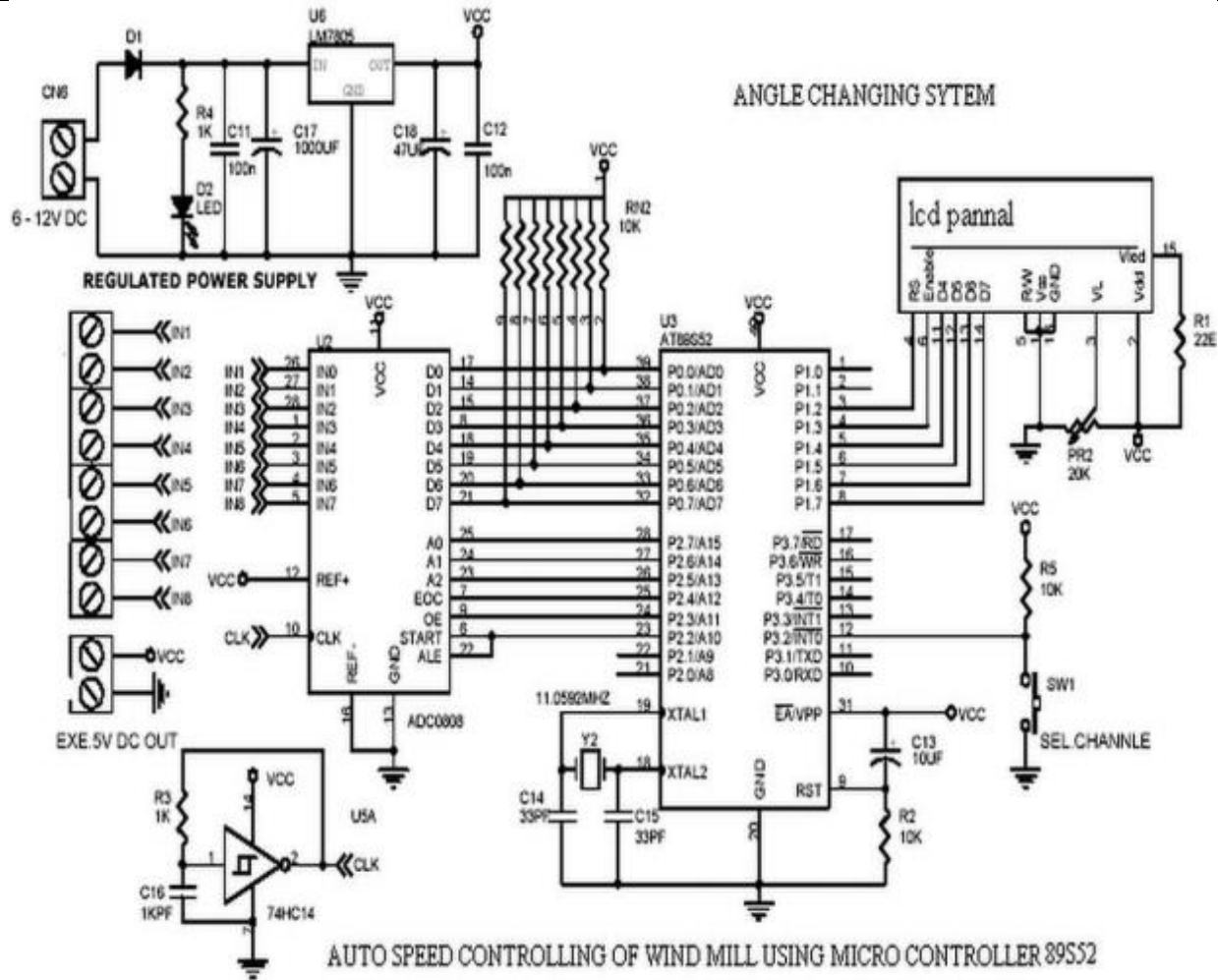


Fig.1 Circuit Diagram and Working

The AT89C51 provides the following standard features: 4K bytes of Flash, 128 bytes of RAM, 32 I/O lines, two 16-bit timer/counters, a five vector two-level interrupt architecture, a full duplex serial port, on-chip oscillator and clock circuitry. In addition, the AT89C51 is designed with static logic for operation down to zero frequency and supports two software selectable power saving modes. The Idle Mode stops the CPU while allowing the RAM, timer/counters, serial port and interrupt system to continue functioning. The Power down Mode saves the RAM contents but freezes the oscillator disabling all other chip function until the next hardware reset.

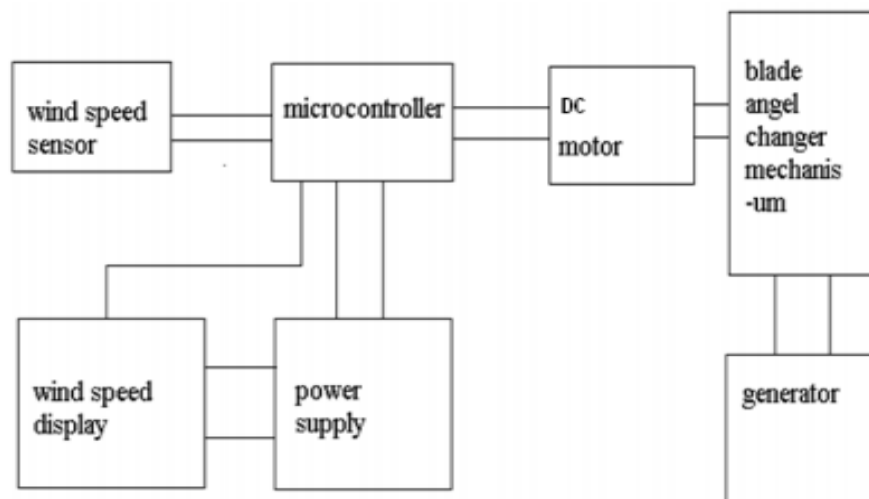


Fig.2 Block Diagram for individual Pitch Control

Normally analog-to-digital converter (ADC) needs interfacing through a chip to change over analog data into digital format. This requires hardware and necessary software, bringing about increased intricacy and thus the total cost. The circuit of A-to-D converter appeared here is designed around ADC 0808, avoiding the utilization of a chip. The ADC 0808 is a 8-bit A-to-D converter, having data lines D0-D7. It takes a shot at the standard of progressive approximation. It has a total of eight analog information channels, out of which any one can be chosen utilizing address lines A, B and C. Here, in this case, input channel IN0 is chosen by establishing A, B and C address lines. Usually the control signals EOC (end of change), SC (start transformation), ALE (address latch enable) and OE (yield enable) are interfaced by means of a microchip. Be that as it may, the circuit appeared here is worked to operate in its nonstop mode without utilizing any chip. Subsequently the information control signals ALE and OE, being active-high, are fixing to Vcc (+5 volts). The information control signal SC, being active-low, initiates start of transformation at falling edge of the beat, whereas the yield signal EOC turns out to be high after fruition of digitization. This EOC yield is coupled to SC enter, where falling edge of EOC yield acts as SC contribution to coordinate the ADC to start the change. As the transformation starts, EOC signal goes high. At next clock beat EOC yield again goes low, and consequently SC is enabled to start the following transformation. Hence, it gives persistent 8-bit digital yield comparing to instantaneous value of analog information. The maximum level of analog information voltage ought to be appropriately scaled down underneath positive reference (+5V) level. The ADC 0808 IC requires clock signal of typically 550 kHz, which can be easily gotten from an as table multi vibrator, developed utilizing 7404 inverter gates. Keeping in mind the end goal to visualize the digital yield, the column of eight LEDs (LED1 through LED8) have been utilized, wherein each LED is associated with individual data lines D0 through D7. Since ADC works in the ceaseless mode, it displays digital yield as soon as analog info is applied.

At the point when the generator is creating power, it causes a torque, contrary to the mechanical torque of the rotor. The MP-controller based completely automatic frameworks controls the created powers, so the rotor speed is kept constant inside a narrow band, which is called slip, which is the prudential relation amongst actual and synchronous rotating speed and optimal adjustment of the angle of the blade in relation to the prevailing twist, along these lines generating maximum power.

V. RESULT ANALYSIS

Wind Shear Correction- No correction needs to be applied to the wind speed-reading for anemometer heights different from hub height. Correction of Power for Air Density Variations Before data analysis using the method of bins is carried out, corrections to the data sets for air density variations must be applied. In this procedure, the wind speed range of operation of the wind turbine is divided into a series of intervals (bins). The aim of the corrections is to bring the power curve and the calculated mean power as close as possible to the values which would be obtained if the measurements were all carried out at a standard air density at sea level of 1.225 Kg / m³ (1013.3 mbar, dry air, 15.15 degree Celsius or 288.15 degrees Kelvin).

For a stall-controlled wind turbine, each 10 min average net power values shall be corrected by applying the following formula: $P_s = P_T [1.22V P_t]$ (4.5)

where,

P_s = Power corrected to standard conditions, P_T = Uncorrected average power, p_T = Test air density and P_T is calculated from 288.15 degrees Kelvin.

where,

B = Barometric pressure, (mbar)

$T = t + 273.15$ and

t = Air temperature in degrees Celsius.

For a pitch-regulated WTG, the correction is the same as for a stall controlled WTG as long as the measured power levels are below 70 % of rated power. For measured power levels above 70 % of rated power, the correction applies instead to wind speed (and not to power) according to the following expression.

$$V = v_t [p_t/1.225]^{1/3} \quad (4.7)$$

Where V_t is the measured, uncorrected wind speed (m / s) and V_s is the wind speed corrected to standard conditions. The ensemble averages (V_i , P_i) are then plotted and a curve fitted through the plotted points. This curve is the WT power curve. The minimum conditions of shorter pre-averaging time does not reduce the total time, as the number of data sets per bin multiplied by the pre averaging time shall be constant and must be met before the curve is established. The power curve is a linearly scaled Cartesian coordinate system graph of WT net power corrected for air density variations (ordinate) versus wind speed (abscissa) as shown in Figure. Both scales start at zero. The ordinate scale should extend to at least 110 % of the WT maximum power. The abscissa should extend to a wind speed of at least 20 meters / second.

The power curve is to be displayed graphically as indicated in Figure 4.11 and in form of a table as shown in Table 4.1. Care should be taken not to apply air density corrections to fractions of the power, which are not dependent on air density, such as gearbox and generator losses. If, for instance, the relation between net power P and rotor power P_R is of the form $P = aP_R - 0$ (4.9) With a and P constant, then the correction of power for air density variations should be $P_s = 1.22VP_t$ ($< *P_R - P$) This will be the case with grid-connected, constant speed WTG, where the electric losses normally will be proportional to the power produced, while the mechanical losses in the drive train will be rotor speed dependent and hence constant for a constant speed WTG.

VI. CONCLUSION

In this paper the strategy for wind turbine controller design was displayed. Summarizing, the control strategy of wind turbines would be ideal if the extracted vitality for each wind speed is maximal. This is hard to achieve, especially when the wind speed is lower (or Higher) than rated. The approach proposed in this paper utilized of designing a controller based on the utilization of artificial insight specifically algorithm hereditary qualities. The simulation comes about speak to that when the wind speed changes, this designed controller can achieve constant yield power and constant rotation speed of wind turbines; it has better dynamic performances.

REFERENCES

- [1] Salami, M., Cain, G., "The Quest for a New Computing Architecture Based on Genetic Algorithms", Proceedings of the Electrical Engineering Congress (EEC94), Sydney, Australia, November 1994.
- [2] Salami, M., Cain, G., "An Adaptive Control System Based on Genetic Algorithms", Proceedings of the FLAIRS-95 International Workshop on Intelligence Adaptive Systems (IAS-95), Melbourne Beach, Florida USA, April 1995.
- [3] Salami, M., Cain, G., "Adaptive Hardware Optimization Based on Genetic Algorithms", Proceedings of The Eighth International Conference on Industrial Application of Artificial Intelligence & Expert Systems (IEA95AIE), Melbourne, Australia, June 1999.